Energy Proceedings
Vol 51, 2025
ISSN 2004-2965

Production Prediction and Optimization Combination in Multilayer Commingled CBM System in Eastern Yunnan and Western Guizhou#

Anna Dai [1], Zhiming Wang [1*], Tianhao Huang [1], Xianlu Cai [1]

1 China University of Petroleum-Beijing 18, Fuxue Road, Changping District, Beijing, China 102249

(*Corresponding Author: Zhiming Wang Email: wangzm@cup.edu.cn)

ABSTRACT

The coalbed methane (CBM) reservoirs in eastern Yunnan and western Guizhou have the characteristics of multiple seams superposed, which are commonly exploited by multilayer commingled methods. It is observed that there is crossflow within the reservoir during the development, which impacts the production. To accurately describe the fluid flow law of multilayer CBM co-production, according to the flow mechanism of CBM in composite reservoirs, establish a multilayer combined fluid flow model including crossflow. A numerical simulator based on a fully implicit finite difference solution was developed to analyze the effect of permeability ratio and interlayer pressure differences on production. The results indicate that the numerical simulation results of the established model have a high compliance rate with the fitting results of the field production data, which confirms the validity of the model production prediction in this paper; With the increase of permeability ratio and interlayer pressure difference, the phenomenon of interlayer interference is intensified, the single well production is low, and the degree of reservoir utilization is poor. Differences in the above major influencing factors have resulted in interlayer conflicts and disturbances during combined production. Therefore, the development of CBM reservoirs should select homogeneous multiple coal seams under the same pressure system for co-production as far as possible. The research results provide a theoretical basis for the rational and efficient development of the CBM reservoir, realize quantitative evaluation of multilayered parameters, and have a certain guiding significance for CBM co-production of the reservoir.

Keywords: coalbed methane, multilayer commingled production, production prediction, interlayer crossflow

NONMENCLATURE

Abbreviations	
CBM	Coalbed Methane
Symbols	
B	Volume factor, m^3/m^3
g	Gravitational acceleration, m/s^2
H	Buried depth, m
k	Fluid permeability, mD
k_r	Relative permeability
p	Fluid pressure, MPa
P_L	Langmuir pressure, MPa
p_{wf}	Bottom hole flowing pressure, MPa
r_e	Equivalent well block radius, m
r_w	Wellbore radius, m
s	Skin factor
S	Fluid saturation, %
V_L	Langmuir volume, m^3
μ	Fluid viscosity, mpa·s
ρ	Density, kg/m^3
ϕ	Porosity

1. INTRODUCTION

CBM is commonly characterized by vertical multi-layer stacking due to sedimentation in the formation process [1,2]. For multilayer stacked CBM systems, combined layer drainage can effectively increase the output of a well and reduce the development cost [3]. However, there is the interlayer pressure difference between the reservoirs in the process of discharge and mining, which generates pressure transfer and leads to gas and water crossflow, which has a large impact on the production of CBM wells and is worthy of further study.

Most of the current CBM numerical simulation software focuses on the development of a single coal seam, and there are fewer studies on the fluid flow law of coal-sandstone segments in coal system gas reservoirs

This is a paper for the 16th International Conference on Applied Energy (ICAE2024), Sep. 1-5, 2024, Niigata, Japan.

[4,5]. Aiming at the complexity of the multilayer combined fluid flow problem, Lefkovits [6] established an unstable fluid flow model for multilayer combined reservoirs without considering the interlayer crossflow and derived an analytical solution for the bottom hole flowing pressure. Bourdet [7] developed a theoretical model of multi-reservoir under proposed steady-state flow conditions based on the wellbore reservoir effect and skin factor and plotted the pressure distribution curve. Yonglu Jia [8] derived the solution of the model by Laplace transform based on the multilayer combined mining model established by Bourdet. Jin Huo [9] proposed a mathematical model of fluid flow in a three-layer co-production reservoir with a fixed pressure boundary, obtained the pressure dynamic calculation formula, drew a Dimensionless pressure plate, and analyzed the effect of interlayer crossflow on pressure. Xianmin Zhang [10] constructed a mathematical model of fluid flow from multilayer combined CBM wells and solved the model approximately based on numerical inversion. The majority of existing numerical simulation studies on the production of multilayer CBM wells have focused on interlayer flow problems generated by connecting multiple reservoirs in the wellbore. However, these studies have not considered the crossflow generated by pore connectivity within the adjacent reservoirs, nor have they conducted an in-depth analysis of the change rule of production and its influencing factors.

Therefore, this paper establishes a fluid flow model for coal-sandstone seam mining by introducing the interlayer crossflow, simulates and researches the production law of CBM wells under the multilayer mining method, and clarifies the main controlling factors affecting the gas production of CBM wells, to provide certain references for the multilayer mining of coal strata.

2. METHODOLOGY

2.1 Physical model and assumptions

For CBM reservoirs containing sandstone interbedded layers, combined layer drainage involves multiple scales of mass transfer including desorption, diffusion, fluid flow, and interlayer crossflow [11-16], Wang [1] established a full-process coupled flow model of gas-water two-phase in multi-Coalbed methane reservoirs by comprehensively considering dynamic permeability and crossflow. The physical model is shown in Figure 1.

To facilitate the study, the following basic assumptions are introduced when constructing the three-layer coupled flow model for coal-sandstone seams:

(1) Coal seam is a dual-porosity media containing matrix blocks and fracture networks, and sandstone is a single-porosity system [17-19].

(2) The adsorbed methane is desorbed from the coal matrix surface into the matrix and enters the fractures by diffusion, and the gas adsorption satisfies the Langmuir equation [20-24].

(3) The flow of fluids through the fractures of both coal and sandstone seams is Darcy flow.

(4) Fluid flows between coal and sandstone seams in the form of crossflow.

(5) Neglecting the effect of capillary forces and the dissolution of CBM in water.

(6) The temperature is constant during flow.

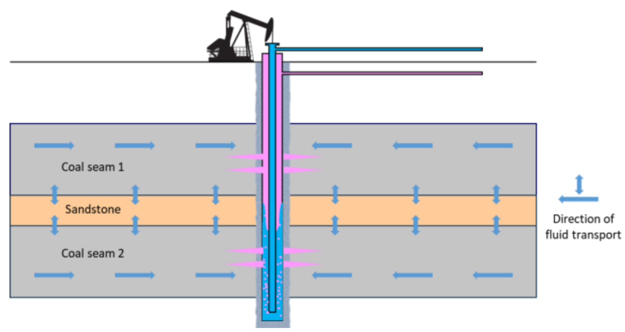

Fig. 1 Multilayer CBM well fluid flow physical model

2.2 *Mathematical model and solution*

A mathematical model applicable to multilayer collocated mining is established and solved, which concluded that the formation pressure is decreased by drainage, and the methane is desorbed from the matrix and then diffuses into the fracture driven by the concentration gradient, generating fluid exchange with the sandstone layers, and finally entering the wellbore output by fluid flow.

2.2.1 Mathematical modeling

The flow equations in the coal seam fracture are as follows:

$$\nabla\left[\frac{k^{cf}k_{rg}^{cf}}{\mu_g^{cf}B_g^{cf}}\nabla\left(p_g^{cf}-\rho_g^{cf}gH^c\right)\right]+\Delta q_{gcross}^c+q_{gmf}^c-q_{gwell}^c=\frac{\partial}{\partial t}\left(\frac{S_g^{cf}\phi^{cf}}{B_g^{cf}}\right) \quad (1)$$

$$\nabla\left[\frac{k^{cf}k_{rw}^{cf}}{\mu_w^{cf}B_w^{cf}}\nabla\left(p_w^{cf}-\rho_w^{cf}gH^c\right)\right]+\Delta q_{wcross}^c-q_{wwell}^c=\frac{\partial}{\partial t}\left(\frac{S_w^{cf}\phi^{cf}}{B_w^{cf}}\right) \quad (2)$$

Where the superscript cf is the coal fracture system, c is the coal seam; the subscript g is the gas phase, w is the water phase; Δq_{gcross}^c and Δq_{wcross}^c are the crossflow rate of gas and water between the coal seam and sandstone, m^3/d; q_{gmf}^{c} is the desorption volume of CBM, m^3/d; q_{gwell}^{c} and q_{wwell}^{c} are the production of gas and water, m^3/d.

The gas is mainly in the adsorption state in the coal seam, and during the development process, the gas is gradually desorbed as the pressure decreases. The amount of desorption can be expressed as:

$$q_{gmf}^{c}\Big|^{n+1} = \frac{V_a\big|^{n} - V_a\big|^{n+1}}{\Delta t} \tag{3}$$

Where $q_{gmf}^{c}\big|^{n+1}$ is the desorption volume of CBM at time $n+1$, m^3/d; $V_a\big|^{n}$ is the adsorption volume at time n, m^3; $V_a\big|^{n+1}$ is the adsorption volume at time $n+1$, m^3; Δt is time-varying quantity, d.

The adsorption of gases in the matrix micropores satisfies the Langmuir equation and can be expressed as [25]:

$$V_a\Big|^{n} = \frac{V_L p_g^{cf}\big|^{n}}{p_g^{cf}\big|^{n} + p_L} \tag{4}$$

Similarly, the transport equation in the pores of the sandstone layer can be obtained as:

$$\nabla\left[\frac{k^s k_{rg}^s}{\mu_g^s B_g^s}\nabla\left(p_g^s - \rho_g^s g H^s\right)\right] + \Delta q_{gcross}^{s} - q_{gwell}^{s} = \frac{\partial}{\partial t}\left(\frac{S_g^s \phi^s}{B_g^s}\right) \tag{5}$$

$$\nabla\left[\frac{k^s k_{rw}^s}{\mu_w^s B_w^s}\nabla\left(p_w^s - \rho_w^s g H^s\right)\right] + \Delta q_{wcross}^{s} - q_{wwell}^{s} = \frac{\partial}{\partial t}\left(\frac{S_w^s \phi^s}{B_w^s}\right) \tag{6}$$

Where the superscript s is the sandstone pore system; Δq_{gcross}^{s} and Δq_{wcross}^{s} are the crossflow rate of gas and water between the sandstone and coal seam, m^3/d; q_{gwell}^{s} and q_{wwell}^{s} are the production of gas and water, m^3/d.

Due to the different physical properties of coal and sandstone seams, there is often a pressure difference between the layers [26], and the pressure difference produces material exchange, and the amount of interlayer crossflow is:

$$\Delta q_{gcross}^{c} = -\Delta q_{gcross}^{s} = \sigma \frac{k^{cf} k_{rg}^{cf}}{\mu_g^{cf} B_g^{cf}}\left(p_g^{cf} - p_g^{s}\right) \tag{7}$$

$$\Delta q_{wcross}^{c} = -\Delta q_{wcross}^{s} = \sigma \frac{k^{cf} k_{rw}^{cf}}{\mu_w^{cf} B_w^{cf}}\left(p_w^{cf} - p_w^{s}\right) \tag{8}$$

Where $\sigma = \frac{4}{h^2}$ is the geometric factor, m^{-2}.

In order to completely describe the transport process of gas and water and to solve equations, it is also necessary to introduce auxiliary equations and definite conditions.

$$\begin{cases} q_{well} = \dfrac{\sqrt{k_x k_y} k_r}{\mu B}\dfrac{2\pi h}{\ln\left(r_e / r_w\right) + s}\left(p - p_{wf}\right) \\ \left.\dfrac{\partial p}{\partial x}\right|_{x=0,L} = 0 \\ \left.\dfrac{\partial p}{\partial y}\right|_{y=0,W} = 0 \\ \left.\dfrac{\partial p}{\partial z}\right|_{z=0,H} = 0 \\ p\left(x,y,z,t\right)\big|_{t=0} = p_0\left(x,y,z\right) \\ S\left(x,y,z,t\right)\big|_{t=0} = S_0\left(x,y,z\right) \end{cases} \tag{9}$$

The calculation of r_e introduces the concept of effective wellbore diameter defined by Peaceman:

$$r_e = 0.28\frac{\left[\left(k_y / k_x\right)^{0.5}\Delta x^2 + \left(k_x / k_y\right)^{0.5}\Delta y^2\right]^{0.5}}{\left(k_y / k_x\right)^{0.25} + \left(k_x / k_y\right)^{0.25}} \tag{10}$$

Where k_x and k_y are the directional permeability of x and y, mD; Δx and Δy are the mesh size in x and y direction, m.

2.2.2 Solution of the mathematical model

The gas-water two-phase full-process coupled flow model developed above is a complex set of nonlinear partial differential equations. Based on this, the established mathematical model needs to be finite difference processed.

Taking the gas-phase flow equation in a coal seam as an example, a finite difference discretization of Eq. (1) is performed, where the superscript cf is omitted and the difference subscripts are in an abbreviated form in the processing, e.g. $i+\frac{1}{2} = i+\frac{1}{2}, j, k$.

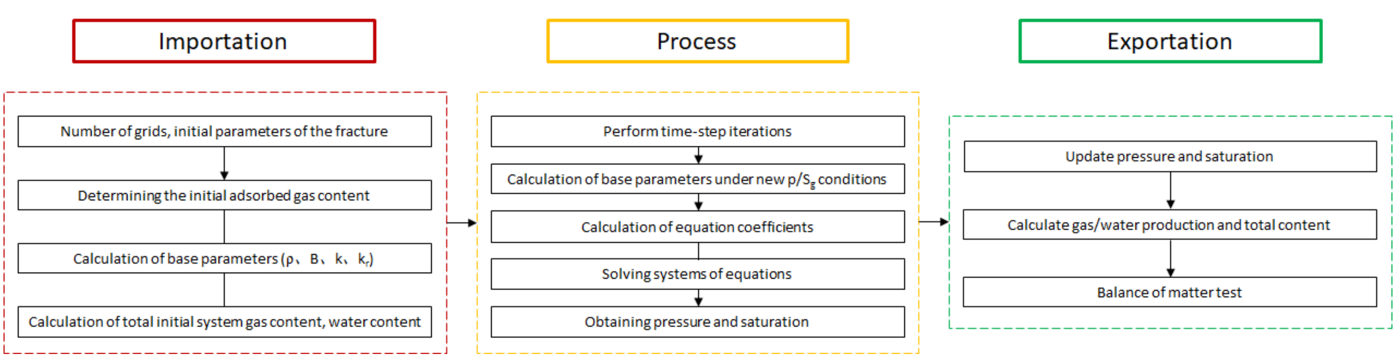

Fig. 2 Flowchart of the CBM simulator

Define the specific weight, mobility, conduction coefficient, and second-order difference quotient operators as shown in Eq. (11), (12), (13), and (14):

$$\gamma_g = \rho_g g \tag{11}$$

$$\lambda_g = \frac{kk_{rg}}{\mu_g B_g} \tag{12}$$

$$\begin{cases} T_{xg\left(i+\frac{1}{2}\right)} = \dfrac{\Delta y_j \Delta z_k}{\Delta x_{i+\frac{1}{2}}} \lambda_{g\left(i+\frac{1}{2}\right)},\ T_{xg\left(i-\frac{1}{2}\right)} = \dfrac{\Delta y_j \Delta z_k}{\Delta x_{i-\frac{1}{2}}} \lambda_{g\left(i-\frac{1}{2}\right)} \\ T_{yg\left(j+\frac{1}{2}\right)} = \dfrac{\Delta x_i \Delta z_k}{\Delta y_{j+\frac{1}{2}}} \lambda_{g\left(j+\frac{1}{2}\right)},\ T_{yg\left(j-\frac{1}{2}\right)} = \dfrac{\Delta x_i \Delta z_k}{\Delta y_{j-\frac{1}{2}}} \lambda_{g\left(j-\frac{1}{2}\right)} \\ T_{zg\left(k+\frac{1}{2}\right)} = \dfrac{\Delta x_i \Delta y_j}{\Delta z_{k+\frac{1}{2}}} \lambda_{g\left(k+\frac{1}{2}\right)},\ T_{zg\left(k-\frac{1}{2}\right)} = \dfrac{\Delta x_i \Delta y_j}{\Delta z_{k+\frac{1}{2}}} \lambda_{g\left(k-\frac{1}{2}\right)} \end{cases} \tag{13}$$

$$\begin{cases} \Delta_x T_{xg} \Delta_x p_g = T_{xg\left(i+\frac{1}{2}\right)} \left(p_{gi+1} - p_{gi}\right) - T_{xg\left(i-\frac{1}{2}\right)} \left(p_{gi-1} - p_{gi}\right) \\ \Delta_y T_{yg} \Delta_y p_g = T_{yg\left(j+\frac{1}{2}\right)} \left(p_{gj+1} - p_{gj}\right) - T_{yg\left(j-\frac{1}{2}\right)} \left(p_{gj-1} - p_{gj}\right) \\ \Delta_z T_{zg} \Delta_z p_g = T_{zg\left(k+\frac{1}{2}\right)} \left(p_{gk+1} - p_{gk}\right) - T_{zg\left(k-\frac{1}{2}\right)} \left(p_{gk-1} - p_{gk}\right) \end{cases} \tag{14}$$

Using block centered grid system, the difference equation for the point (i, j, k, n+1) is:

$$\begin{aligned} &\Delta_x T_{xg} \Delta_x p_g \Big|^{n+1} + \Delta_y T_{yg} \Delta_y p_g \Big|^{n+1} + \Delta_z T_{zg} \Delta_z p_g \Big|^{n+1} \\ &- \Delta_x T_{xg} \gamma_g \Delta_x H^c - \Delta_y T_{yg} \gamma_g \Delta_y H^c - \Delta_z T_{zg} \gamma_g \Delta_z H^c \\ &+ \Delta q_{gcross} V_{ijk} + q_{gmf} V_{ijk} - q_{gwell} V_{ijk} = \frac{V_{ijk}}{\Delta t} \left[\left(\frac{S_g \phi}{B_g} \right) \Bigg|^{n+1} - \left(\frac{S_g \phi}{B_g} \right) \Bigg|^{n} \right] \end{aligned} \tag{15}$$

Define again as follows:

$$\Delta T_g \Delta p_g \Big|^{n+1} = \Delta_x T_{xg} \Delta_x p_g \Big|^{n+1} + \Delta_y T_{yg} \Delta_y p_g \Big|^{n+1} + \Delta_z T_{zg} \Delta_z p_g \Big|^{n+1} \tag{16}$$

$$\Delta T_g \gamma_g \Delta H^c = \Delta_x T_{xg} \gamma_g \Delta_x H^c + \Delta_y T_{yg} \gamma_g \Delta_y H^c + \Delta_z T_{zg} \gamma_g \Delta_z H^c \tag{17}$$

$$Q = \Delta q_{gcross} + q_{gmf} - q_{gwell} \tag{18}$$

Eq. (15) can be simplified as:

$$\Delta T_g \Delta p_g \Big|^{n+1} - \Delta T_g \gamma_g \Delta H^c + Q V_{ijk} = \frac{V_{ijk}}{\Delta t} \left[\left(\frac{S_g \phi}{B_g} \right) \Bigg|^{n+1} - \left(\frac{S_g \phi}{B_g} \right) \Bigg|^{n} \right] \tag{19}$$

The Newton-Raphson iterative fully implicit equations are used to solve the above discrete equations to obtain a multilayer commingled simulator for CBM reservoirs. The schematic of the simulator solution is shown in Figure 2.

3. MODEL AND ALGORITHM VALIDATION

The reliability of the mathematical model and simulator is verified by comparing and analyzing the actual production data. The input parameters of the simulator are shown in Table 1. The comparison results of CBM production are shown in Figure 3, and the simulator calculation results have good consistency with the production data, which preliminarily verifies the reliability of the simulator.

Figure 4 illustrates that the production considering crossflow is smaller than ignoring crossflow. Furthermore, the longer the time, the larger the difference between the two.

Table 1 Simulator validation of input parameters

Adsorption	Value	Coal seam fracture	Value	Sandstone	Value
Langmuir pressure/MPa	2.5	Pressure/MPa	9	Pressure/MPa	10
Langmuir volume/m^3	3E5	Porosity/%	7	Porosity/%	5
Critical desorption pressure/MPa	5.8	Permeability/mD	0.5	Permeability/mD	0.02
Desorption time/d	10	Water saturation/%	99.9	Water saturation/%	99

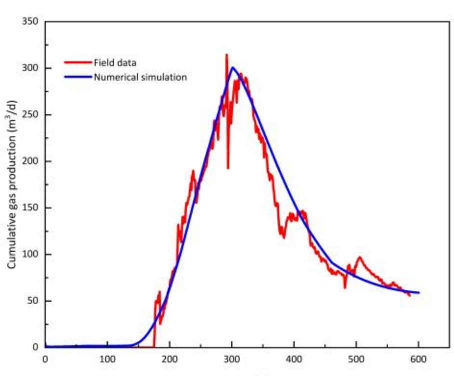

Fig. 3 Comparison of field data and simulation results

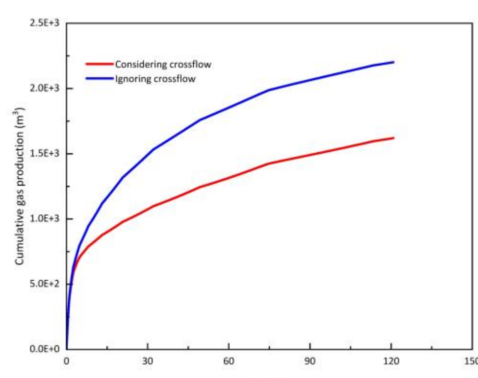

Fig. 4 Cumulative gas production curve considering/ignoring interlayer crossflow

After 120 days, the cumulative production decreased by 25 %, which can be attributed to the higher permeability of the coal seam compared to that of the sandstone. This results in the gas flowing from the sandstone to the coal seam, reducing the pressure drop within the coal seam. Consequently, the interlayer crossflow cannot be disregarded when conducting a prediction of the CBM production.

4. ANALYSIS OF INFLUENCING FACTORS

Two important factors affecting the combined production, permeability ratio, and reservoir pressure difference, were selected as research objects for sensitivity analysis, and the specific parameter settings are shown in Table 2.

Permeability ratio m refers to the ratio of the maximum permeability to the minimum permeability of the main producing seams (Coal seam 1 and Coal seam 2), and reservoir pressure difference n refers to the difference in pressure between adjacent seams.

$$m = \frac{k_{\max}}{k_{\min}} \qquad n = p_{down} - p_{up} \tag{20}$$

Table 2 Parameter values for sensitivity analysis

Permeability/mD				Pressure/MPa			
Coal seam 1	Sandstone	Coal seam 2	m	Coal seam 1	Sandstone	Coal seam 2	n
0.5	0.02	0.5	1	9	9.5	10	0.5
0.8	0.02	0.2	4	8	9	10	1
0.9	0.02	0.1	9	7	8.5	10	1.5

4.1 Effect of permeability ratio

In order to study the effect of reservoir inhomogeneity on gas well production, a combined mining model was established by considering the permeability ratio of the main producing seams (Coal seam 1 and Coal seam 2) to be 1, 4, and 9, respectively, while ensuring the same average permeability.

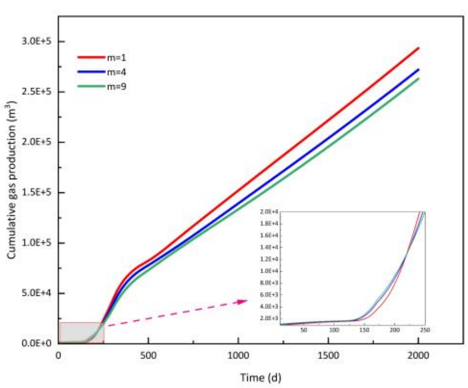

Fig. 5 Cumulative gas production curves with different permeability ratio

As can be seen from Figure 5, in the early stage of production, the permeability ratio has less influence on fluid flow, which is because at this time, coal seam 1 is the main production layer, and the production is affected by the permeability of a single layer. As the gas reservoir pressure gradually decreases to the critical desorption pressure, the adsorbed gas in the coal seam begins to desorb, resulting in an upward curve of cumulative production. The contribution of coal seam 2 to the production begins to appear, and the cumulative production of gas wells decreases with the increase of permeability ratio, and the phenomenon of interlayer interference increases.

In order to further analyze the result, the plan view of the pressure distribution of coal seam 1, sandstone and coal seam 2 at the discharge time of 1000d was plotted. Comparing the results of pressure drop funnels of coal seam 1 under different permeability ratio, it can be seen that with the increase of permeability ratio, the initial permeability of coal seam 1 is larger, the pressure drop transfer rate of this layer is faster, the transfer range is larger, and it is easy to form deeper pressure drop funnels at the wellbore, which leads to the increase of gas production from this layer.

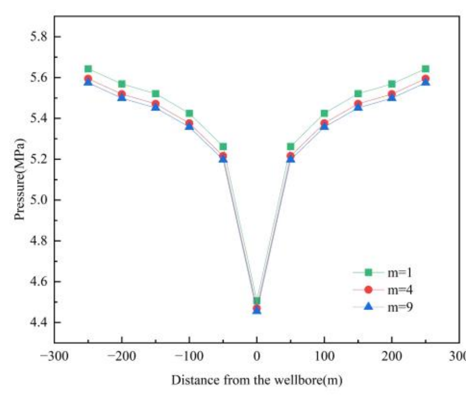

Fig. 6 Variation of pressure in coal seam 1 with different permeability ratio (Time=1000d)

However, as the permeability of coal seam 1 increases, the pressure drop of coal seam 2 reservoir is smaller, and the pressure drop funnel becomes more difficult to expand. This is because under the condition of certain drainage, with the increase of permeability of

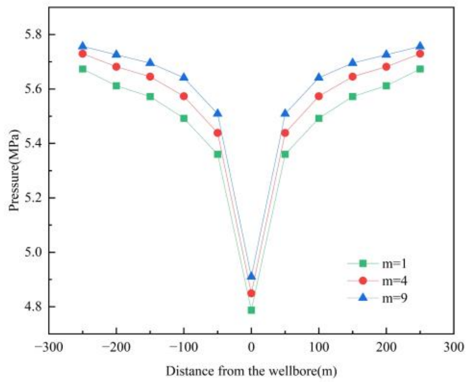

Fig. 7 Variation of pressure in coal seam 2 with different permeability ratio (Time=1000d)

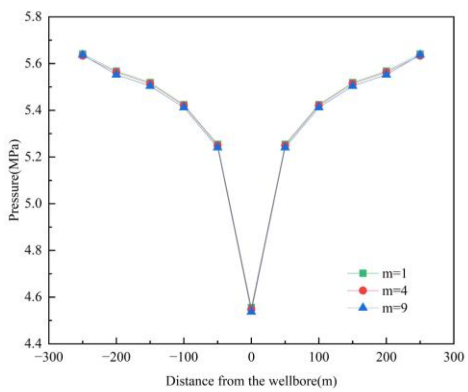

Fig. 8 Variation of pressure in sandstone with different permeability ratio (Time=1000d)

coal seam 1, the drainage in the layer increases, which leads to the decrease of drainage in the adjacent layer, the pressure drop is smaller, and the production capacity is suppressed, thus causing the total gas production to decrease. Meanwhile, as the sandstone layer is a low-permeability section, the permeability grade difference has little effect on the low-permeability section, and the pressure drop funnel is almost unchanged.

In summary, the permeability ratio mainly affects the combined production capacity through pressure drop. The initial permeability has a positive effect on the production capacity of this layer, which is manifested in the fact that the larger the permeability is, the larger the single-layer production is. However, the initial permeability has an inhibitory effect on the neighboring layers, and the larger the permeability is, the more obvious the inhibitory effect is, thus causing the total production capacity to decline. Therefore, the existence of interlayer interference phenomenon should be considered in the development process, and the combination of layers with the same physical properties should be mined as far as possible.

In order to quantitatively analyze the degree of interlayer interference in multi-layer combined mining in CBM reservoirs, the single mining index J_i, the combined mining index J, and the dimensionless interlayer interference coefficient λ are defined, respectively.

$$J_i = \frac{Q_{sgi}}{p_{ei} - p_{wfi}} \qquad J = \sum_{i=1}^{3} \frac{Q_{cgi}}{p_{ei} - p_{wf}} \tag{21}$$

$$\lambda = \frac{J}{\sum_{i=1}^{3} J_i} \tag{22}$$

Where the Q_{sgi} is the gas production when the layer is extracted alone, m^3/d ; the Q_{cgi} is the gas production when the layers are extracted together e, m^3/d .

The interlayer interference coefficient describes the degree of release of gas recovery capacity of multi-layer gas wells, and the smaller its value, the more serious the interlayer interference phenomenon. In this study, 0.5 is used as the limit of interlayer interference in multi-layer gas extraction, less than this value indicates that the interlayer conflict is prominent and unsuitable for co-exploitation and development.

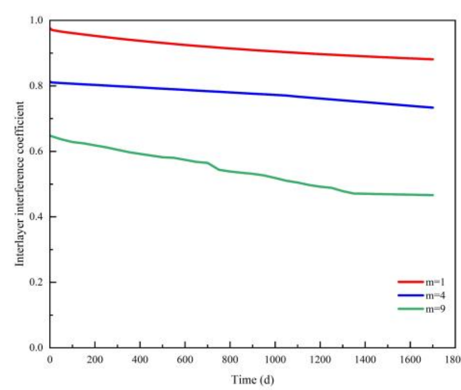

Fig. 9 Variation of interlayer interference coefficient with different permeability ratio

The change of interlayer interference coefficient with production time under different permeability ratio is shown in Fig. 9, which shows that the interlayer interference coefficient decreases with the increase of production time, and the larger the permeability ratio is, the more serious the interlayer interference is. Overall, in the late production period, when the permeability ratio is 1, the interlayer interference coefficient is stable near 0.9, which is suitable for co-mining and development; when the permeability ratio is 4, the interlayer interference coefficient decreases to 0.7, which needs to be considered comprehensively at this time; when the permeability ratio is 9, the interlayer interference coefficient decreases rapidly, and stabilizes at the late stage near 0.45, which is not suitable for co-mining and development.

4.2 Effect of reservoir pressure difference

For multilayer continuous reservoir formation, the pressure systems of neighboring layers are not equal. During the mining process, interlayer interference occurs between high-pressure coal seams and low-pressure coal seams through sandstone interbedding, so the effect of different reservoir pressure differences on gas well production is investigated.

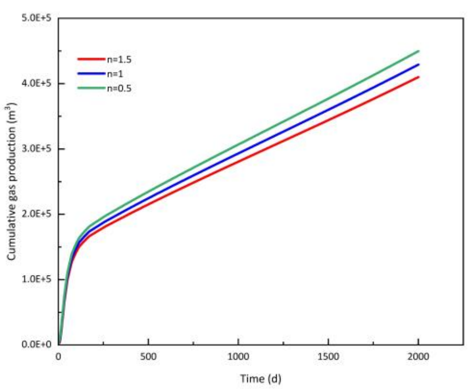

Fig. 10 Cumulative gas production curves with different reservoir pressure difference

As can be seen from Figure 10, in the early stage of production, the influence of interlayer pressure difference on the cumulative gas production is not obvious, which is because at this time, coal seam 1 is the main production layer, and the interlayer interference phenomenon is not yet significant. As production proceeds, the inhibitory effect of the high-pressure coal seam on the low-pressure coal seam is strengthened, and the cumulative production of the gas wells decreases with the increase of the reservoir pressure difference, and the phenomenon f inter-stratum interference is intensified.

Reservoir pressure characterizes the level of energy and also determines the difficulty of development. The smaller the interlayer pressure difference is, the larger the initial pressure of coal seam 1 is. Fig. 11 shows the change of pressure drop of coal seam 1 under different interlayer pressure difference conditions during 1000d of production, which shows that with the increase of initial pressure, the pressure drop funnel is expanding and deepening, which has a promoting effect on the production capacity of this segment.

As coal seam 1 continues to be extracted, the pressure difference between adjacent segments will be more significant, which is manifested in the increase of gas production from coal seam 2. Meanwhile, as the sandstone layer is a low-permeability layer section, the pressure drop funnel changes little.

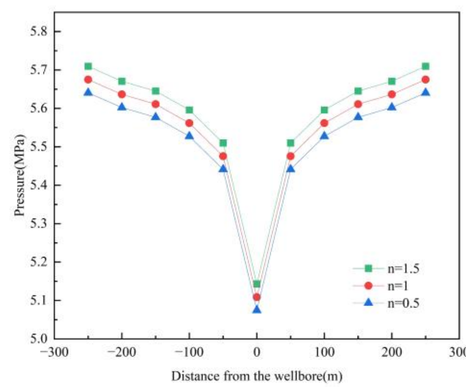

Fig. 11 Variation of pressure in coal seam 1 with different pressure difference (Time=1000d)

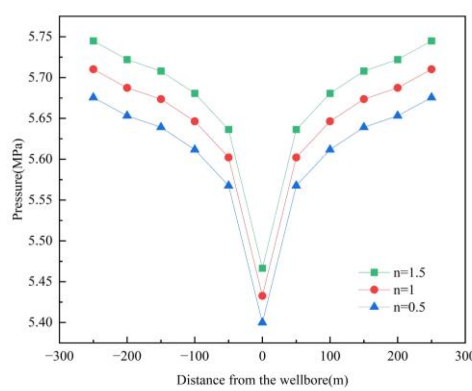

Fig. 12 Variation of pressure in coal seam 2 with different pressure difference (Time=1000d)

In summary, the reservoir pressure difference mainly affects the pressure of coal seam 1. The smaller the interlayer pressure difference is, the reservoir pressure of the first seam section gradually increases, which promotes the total production. Therefore, the size of the interlayer pressure difference should be considered in the process of multi-gas mining, and the gas-bearing layers in the same pressure system should be mined as far as possible.

The change of interference coefficient with production time under different interlayer pressure differences is shown in Figure 14, which shows that the interlayer interference coefficient decreases with the increase of production time, and the larger the interlayer differential pressure is, the more serious the interlayer interference is. When the interlayer pressure difference is 0.5, 1 and 1.5 MPa, the interlayer interference coefficients are 0.88, 0.8, and 0.7, respectively.

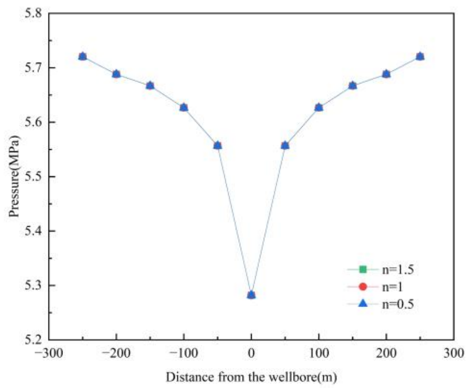

Fig. 13 Variation of pressure in sandstone with different pressure difference (Time=1000d)

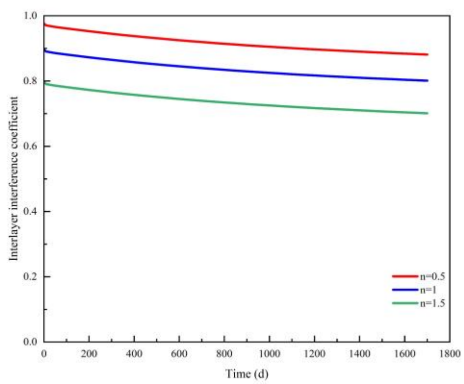

Fig. 14 Variation of interlayer interference coefficient with different pressure difference

5. CONCLUSIONS

The interlayer crossflow was introduced to establish a multilayer combined mining fluid flow model for CBM reservoirs, and the reliability of the model was verified by comparing it with examples, and the relationship between the permeability ratio and reservoir pressure difference and the production of the combined wells was investigated respectively, and the conclusions obtained are as follows.

(1) A mathematical model of fluid flow in multilayer combined CBM reservoirs was constructed, and a numerical simulator based on the finite-difference method was developed, which was verified by comparing with well data to achieve an accurate characterization of fluid transport in multilayer combined CBM reservoirs.

(2) For heterogeneous reservoirs, the influence of heterogeneity on the production of joint extraction wells cannot be ignored. Under the condition of the same average permeability, the larger the permeability ratio, the smaller the yield, the more intense the interlayer interference, and the worse the degree of reservoir mobilization. Permeability ratio is proportional to the intensity of interference, permeability ratio is greater than 9, the interlayer interference coefficient is reduced to less than 0.5, which is not suitable for co-mining and development.

(3) For composite reservoirs, the interlayer pressure difference causes fluid transport between different reservoirs, the larger the interlayer pressure difference, the smaller the yield, and the degree of interlayer interference is intensified, so it is recommended to select multiple coal seams with the same pressure system for combined mining. The interlayer pressure difference is positively proportional to the interference intensity, and the interlayer pressure difference is within 1MPa, which is suitable for co-mining and development.

ACKNOWLEDGEMENT

The authors gratefully acknowledge the financial support provided by the National Natural Science Foundation of China [grant number 51974333].

DECLARATION OF INTEREST STATEMENT

The authors declare that they have no known competing financial interests or personal relationships that could have an impact on the work reported in this paper.

REFERENCE

[1] Wang, Z.M., Zeng, Q.S., Zhang, J. Fundamental Theory of Coalbed Methane Development. 2021:153–155.

[2] Qin, Y., Shen, J., Shen, Y.L. Joint mining compatibility of superposed gas-bearing systems: a general geological problem for extraction of three natural gases and deep CBM in coal series. J. China Coal Soc. 2016, 41 (1):14–23. DOI: 10.13225/j.cnki.jccs.2015.9032

[3] Pashin, J.C. Variable gas saturation in coalbed methane reservoirs of the Black Warrior Basin: impl ications for exploration and production. Int. J. Coal Geol. 2010, 82:135-146. DOI: 10.1016/j.coal.2009.10. 017

[4] Xu, H., Qin, Y.P., Wu, F., Zhang, F.J., Liu, W., Liu, J., Guo, M.Y. Numerical modeling of gas extraction from coal seam combined with a dual-porosity model: Finite difference solution and multi-factor analysis. Fuel. 2022, 313,122687. DOI: 10.1016/j.fuel.2021.122687

[5] Lanetc, Z., Zhuravljov, A., Tang, K., Armstrong, R. T., Mostaghimi, P. Multi-scale modelling of multi-physics flow in coal seams. J. Nat Gas Sci Eng. 2023, 118,205081. DOI: 10.1016/j.jgsce.2023.205081

[6] Lefkovits, H.C., Hazebroek, P., Allen, E.E. A Study of the Behavior of Bounded Reservoirs Composed of Stratified Layers. SPE J. 1961, 1(1):43-58. DOI: 10.2118/1329-G

[7] Bourdet, D. Pressure Behavior of Layered Reservoirs With Crossflow.Paper presented at the SPE California Regional Meeting, Bakersfield, California, March 1985. DOI: 10.2118/13628-MS

[8] Jia, Y.L., Li, Y., Deng, J.B. Analytical Solution of Bottom Hole Pressure Behavior in Layered Reservoirs with Wellbore Phase Redistribution and Crossflow. J. Southwest Pet. Inst. 1997, (01):49-53+5. DOI: 10.3863/j.issn.1000-2634.1997.01.008

[9] Huo, J., Jia, Y.L., Wang, H.T., Wu, C.Y., Zhang, M. Oil and Gas Reservoir Model for Multilayer Channeling and Dynamic Monitor Down Hole Pressure. J. Well. Test. 2006, (02):1-4+75. DOI: 10.3969/j.issn.1004-4388.2006.02.001

[10] Zhang, X.M., Wu, H.Y., Feng, Q.H., Liu, S., Wu, H.M. Dynamic characteristics of commingled coalbed methane production in wells with multi-layer coal seams. J. China Univ. Pet., Ed. Nat. Sci. 2020, 44(06):88-96. DOI: 10.3969/j.issn.1673-5005.2020.06.011

[11] Li, Z.W., Yu, H.J., Bai, Y.S., et al. Analysis of reservoir permeability evolution and influencing factors during CO_2-Enhanced coalbed methane recovery. ENEYDS. 2024, 304. DOI: 10.1016/j.energy.2024.132045

[12] Liang, S., Liang, Y.W., Elsworth, D., et al. Permeability evolution and production characteristics of inclined coalbed methane reservoirs on the southern margin of the Junggar Basin, Xinjiang, Int. J. Rock Mech. Min Sci. 2023, 171. DOI: 10.1016/j.ijrmms.2023.105581

[13] Sun, X.N., Hu, S.Y., Chen, Z.Y., et al. Permeability enhancement of coal-bearing propped fractures using blockage removal agent treatments in coalbed methane reservoirs. ENEYDS. 2024, 124. DOI: 10.1016/j.jgsce.2024.205259

[14] Sun, F.R., Liu, D.M., Cai, Y.D., et al. Vector characteristics of microscale gas transport in coalbed methane reservoirs. Gas Sci. Eng. 2023, 118. DOI: 10.1016/j.jgsce.2023.205085

[15] Lu, Y., Kang, Y.L., Ramakrishna, S., et al. Enhancement of multi-gas transport process in coalbed methane reservoir by oxidation treatment: Based on the change of the interaction force betweencoal matrix and gas molecules and knudsen number. Int. J. Hydrogen Energy. 2023, 48(2):478-494. DOI: 10.1016/j.ijhydene.2022.09.265

[16] Zhang, J.C., Bian, X.B. Numerical simulation of hydraulic fracturing coalbed methane reservoir with independent fracture grid. Fuel. 2015, 143:543-546. DOI: 10.1016/j.fuel.2014.11.070

[17] Xu, H., Qin, Y.P., Wu, F., et al. Numerical modeling of gas extraction from coal seam combined with a dual-porosity model: Finite difference solution and multi-factor analysis. Fuel. 2022, 313. DOI: 10.1016/j.fuel.2021.122687

[18] Shi, G.S., Wei, F.Q., Gao, Z.Y., et al. Gas desorption-diffusion behavior from coal particles with consideration of quasi-steady and unsteady crossflow mechanisms based on dual media concept model: Experiments and numerical modelling. Fuel. 2021, 298. DOI: 10.1016/j.fuel.2021.120729

[19] Thararoop, P., Karpyn, Z.Y., Ertekin, T. Development of a multi-mechanistic, dual-porosity, dual-permeability, numerical flow model for coalbed methane reservoirs. J. Nat. Gas Sci. Eng. 2012, 8:121-131. DOI: 10.1016/j.jngse.2012.01.004

[20] Yang, Y., Liu, S.M., Zhao, W., et al. Intrinsic relationship between Langmuir sorption volume and pressure for coal: Experimental and thermodynamic modeling study. Fuel. 2019, 241:105-117. DOI: 10.1016/j.fuel.2018.12.008

[21] Hao, S.X., Chu, W., Jiang, Q., et al. Methane adsorption characteristics on coal surface above critical temperature through Dubinin–Astakhov model and Langmuir model. Colloids Surf., A. 2014, 444:104-113. DOI: 10.1016/j.colsurfa.2013.12.047

[22] Tang, X., Ripepi, N., Stadie, N.P., et al. A dual-site Langmuir equation for accurate estimation of high pressure deep shale gas resources. Fuel. 2016, 185:10-17. DOI: 10.1016/j.fuel.2016.07.088

[23] Siitonen, J., Sainio, T. Explicit equations for the height and position of the first component shock for binary mixtures with competitive Langmuir isotherms under ideal conditions. J. Chromatography A. 2011, 1218(37):6379-6387. DOI: 10.1016/j.chroma.2011.07.004

[24] Zhang, Z., Liu, G.F., Wang, X.M., et al. A fractal Langmuir adsorption equation on coal: Principle,

methodology and implication. Chem. Eng. J. 2024, 488. DOI: 10.1016/j.cej.2024.150869

[25] Yu, H.G., Zhou, L.L., Guo, W.G., et al. Predictions of the adsorption equilibrium of methane/carbon dioxide binary gas on coals using Langmuir and ideal adsorbed solution theory under feed gas conditions. Int. J. Coal Geol. 2008:73(2), 115-129. DOI: 10.1016/j.coal.2007.03.003

[26] Yang, Z.B., Qin, Y., Chen, S.Y., et al. Controlling mechanism and vertical distribution characteristics of reservoir energy of multi-coalbeds. Acta Geol. Sin. 2013,87(1):139-144. DOI: 10.3969/j.issn.0001-5717.2013.01.014